The Capture of Satellites by Binary-Planet Encounters: A Computational Analysis of the Cases of Triton, Phobos and Deimos

Abstract

Conversely to regular satellites, irregular ones have been widely accepted to be foreign bodies originated elsewhere from their present location, that early in the Solar System history were somehow captured by planets. However, despite almost unanimous agreement about the what and when, the question about how such irregular satellites became gravitationally apprehended by planets remains wide open, as no model seems to satisfactory tie up all loose ends.

A promising capture mechanism has recently been proposed for Triton, the flag-ship of irregular satellites given its huge mass and inclined retrograde motion around Neptune. The key idea of this capture model is based on a three-body gravitational encounter, that is, two bound Kuiper belt objects would have adequately approached Neptune becoming finally disrupted, thus one member resulting captured by the planet – Triton – and the other one liberated.

The aim of this project has been be to investigate by computational analysis the properness of the binary-planet encounter mechanism for explaining the existence of three particular 'hard' cases: Triton, Phobos and Deimos. The weird Triton had been already analyzed, but this time a broader binary characteristic spectrum – both dynamical and physical – have been applied. On the other hand, no previous studies for the case of Martian moons were known.

The obtained results for Triton are in close agreement with published data, while at the same time new wider empirical parameters expanding capture feasibility have been found. Contrarily, results for both Phobos and Deimos have shown capture by binary-Mars encounters almost unviable for the broad range of tried binary characteristics. This poses a big interrogation mark on the binary-planet gravitational encounter model as the potentially flawless and very likely mechanism for explaining all satellite captures in the Solar System.

Introduction

Aside than closest small ring moons, natural satellites can be dynamically divided into two categories. On the one hand 'regular' satellites, which have nearly circular orbits in the equatorial plane of their host planets, orbit in the same direction as planet rotates – prograde motion – and lay at distances of several to tens of planetary radii. On the other hand, 'irregular' satellites, which present different characteristics like large, highly eccentric and/or highly inclined orbits around host planets, orbiting in either direction – prograde or retrograde. Typically regular satellites are large moons, while irregular ones are smaller.

Clearly, dynamic behaviour of irregular satellites denotes an improbable primordial formation process – circumplanetary disk accretion around current parent planets – as regular moons have certainly undergone. While capture is the obvious explanation for the existence of irregular satellites, to know which particular mechanism actually occurred becomes of major importance, since it constraints planet formation models (Jewitt and Sheppard, 2005).

In order to become captured, a passing object must lose a precise amount of its orbital energy so that it can result gravitationally bound to a new master – the largest dominating mass in the vicinity. In case the kinetic energy loss of the passing object were too low, still it could overpass the gravitational potential energy of the system – comprised by the flying object and the planet – and hence no capture at all would result; while if too high, it could end in a direct collision with the planet.

Technically, the privileged status of being "the largest dominating mass in the vicinity" translates as the region around some massive object where accelerations that it provokes on flying-by bodies are much larger than those due to other larger but most distant objects – known as its 'Hill sphere'. Hence, permanent captures of near-by transiting objects by host planets can only take place within corresponding Hill spheres – a necessary but not sufficient condition.

However, there is no agreement on which particular physical process has been the main cause of irregular satellites capture. Three mechanisms have been basically proposed for explaining the required energy dissipation – gas drag, pull-down, and three-body interactions – but none of them satisfactory answer all the interrogations.

The first mechanism, capture by gas drag (Pollack *et al*., 1979), has to do with the deceleration that an object would have experienced while passing through the gas and dust of a primordial circumplanetary nebula. In case such breaking down action resulted precisely enough – neither too low, nor too high – the object would have been finally captured by the planet in question. However, for a passing object to be transformed into satellite this model requires that it should have encountered about its own mass within the nebula, a hard condition to satisfy except for those very small irregulars (Sheppard, 2005).

The second mechanism, pull-down capture (Heppenheimer & Porco, 1977), refers to the situation resulting when a heliocentric object happens to pass close and with a very slow speed relative to a planet – typically in the nearness of a Lagrange point – which at the same time is rapidly increasing its Hill sphere. If such were the case, the otherwise temporary capture could lead to a permanent capture, as the object's low energy could make it unable to escape the new enlarged Hill sphere. Although plausible, this mechanism requires an enlargement of the Hill sphere over a short timescale – either planet's mass increase, Sun's mass decrease or large planet migrations to happen over a few thousand years – a not very likely scenarios (Sheppard, 2005).

Considering that the number of irregular satellites measured to a given size (a reference magnitude ~ 23) is approximately constant for the four giant planets (Jewitt & Sheppard, 2005), neither gas drag, nor pull-down seem to have been the unique capture mechanism for all irregular satellites, since development conditions for Jupiter and Saturn were radically different compared to those for Uranus and Neptune.

The third mechanism, capture through three-body collisional or collisionless interactions (Colombo & Franklin, 1971), implies the right energy dissipation for one or both small interacting objects due to a close approximation within the Hill sphere of a planet. To work efficiently this mechanism requires a large number of passing bodies near the planets, orders of magnitude much larger than presently observed but possible for the early Solar System (Gomes et *al*., 2005; Hahn, 2005). However, a simple and innovative restriction to this general mechanism greatly enriches it: the particular case when an approaching binary system interacts with a planet.

The capturing model by binary-planet encounters

The binary-planet gravitational encounter model for explaining moon's captures is a particular case of a three body collisionless interaction, where the required energy dissipation comes from slow speeds relative to the planet that each one of the binary objects transitorily experience during part of their revolution around the common centre of mass. If the net velocity of a binary member happens to drop below the escape velocity from a planet's gravitational field then it would be captured – at least as long as it remains within the Hill sphere.

Given modern increasing percentage trend of binary systems in the Solar System constituted by small bodies (Stephens and Noll, 2006), binary-planet encounters appear as a very likely explanation for satellite captures (Morbidelli, 2006).

Agnor & Hamilton (2006) have recently presented an analytical description of the binary-planet encounter process, and evaluated it by using numerical simulations for the particular case of binaries encountering Neptune. What follows until the end of this section is a succinct description of their theoretical analysis.

Due to tidal acting forces, three body encounters will effectively provoke binary disruption when its center of mass passes close enough to the planet that the binary separation is about the Hill radius of the binary with respect to the planet. The binary's Hill radius is given by

$$r_{H(bin)} = d_{P-bin}\left(\frac{m_1 + m_2}{3M_P}\right)^{1/3} \qquad \{1\}$$

where d_{P-bin} is the distance from the binary's center of mass to the planet, and m_1, m_2, M_P are respectively the mass of each binary component and the mass of the planet. Hence, the binary disruption will occur when $r_{H(bin)}$ equals a_{bin} (the binary semi-major axis), in which case the tidal disruption distance becomes

$$r_{td} = a_{bin}\left(\frac{3M_P}{m_1 + m_2}\right)^{1/3} = R_P\left(\frac{a_{bin}}{R_1}\right)\left[\left(\frac{3\rho_P}{\rho_1}\right)\left(\frac{m_1}{m_1 + m_2}\right)\right]^{1/3} \qquad \{2\}$$

where M_P, R_P, ρ_P are respectively the mass, radius, and density of the planet, as well as m_1, R_1, ρ_1 represent the same for the larger binary member, while m_2 is the mass of the smaller one. Realizing that for usual values (roughly $\rho_P \approx \rho_1$, $m_1 \approx m_2$) the term in square brackets is about one, then

$$r_{td} \approx R_P\left(\frac{a_{bin}}{R_1}\right) \qquad \{3\}$$

Numerical simulations of binary-planet encounters performed by Agnor & Hamilton confirmed this last result as the effective scaling length for binary disruption.

Considered from the planet perspective, the common center of mass of an approaching binary system is moving on a planetocentric hyperbolic trajectory, while both binary members orbit around it. On disruption, the smaller body (m_2) experiences a change in speed about the same of its orbital speed around the binary center of mass – equal to 2π times its semi-major axis divided by its period – so that

$$\Delta v_2 \approx \pm \frac{m_1}{m_1 + m_2} \sqrt{\frac{G(m_1 + m_2)}{a_{bin}}} \qquad \{4\}$$

where G is the universal gravitational constant. From conservation of momentum it becomes $\Delta v_1 = \left(m_2 \middle/ m_1 \right) \Delta v_2$, then

$$\Delta v_1 \approx \pm \frac{m_2}{m_1 + m_2} \sqrt{\frac{G(m_1 + m_2)}{a_{bin}}} \qquad \{5\}$$

This last equation denotes that larger kinetic energy loss values for binary object #1 (the satellite candidate) are potentially obtained from binary systems with small semi-mayor axis and larger massive companion.

Whenever the mass of the planet is much more larger than the mass of the binary system, according to Agnor & Hamilton impulsive transfer from an initial hyperbolic encounter orbit to a final bound elliptical orbit at a particular distance (r) from the planet requires a reduction in speed for the captured object of

$$\Delta v_{cap} = \sqrt{v_\infty^2 + 2GM_P / r} - \sqrt{GM_P (2/r - 1/a_{cap})} \qquad \{6\}$$

where v_∞ is the velocity at infinity of the hyperbolic orbit, and a_{cap} is the semi-major axis of the resulting captured orbit.

Equating equations {5} and {6} it results an expression relating the binary characteristics (m_1, m_2, a_{bin}) to the encounter parameters (v_∞, r) and resulting captured orbits (a_{cap}) for the considered planet (M_P). According to the authors, the further the binary disruption takes place from the planet (the greater the r), the larger the resulting semi-major axis of the captured orbit (a_{cap}).

Also, Agnor & Hamilton state that because the tidal forces that cause binary disruption are maximized when the three bodies are most nearly aligned, preferred relative positions between binary members – binary orbital phases – are selected when disruption occurs, which correspondingly makes that resulting semi-major axis of the captured object also achieve quite similar values.

As previously said, in order to become the capture permanent, the satellite candidate object of the binary system must be transferred to a bound elliptical orbit totally contained within the Hill sphere of the host planet (r_H). Considering that for very high eccentricities the captured object will be flying far away at most as almost two semi-major axes from the planet, then

$$a_{cap} \leq \tfrac{1}{2} r_H = \frac{1}{2} a_P \left(\frac{M_P}{3M_S} \right)^{1/3} \qquad \{7\}$$

where a_P is the semi-major axis of the planet's orbit, and M_S is the mass of the Sun.

Once the disrupted binary object has been effectively captured, a new irregular satellite will have been born (most probably, with a large initial eccentricity). In Agnor & Hamilton's own words, *"in principle, this [binary-planet encounter] mechanism can transfer an object to virtually any satellite orbit if the requirements of disruption and capture can be satisfied by the encounter dynamics and the binary characteristics"*.

The SWIFT simulator code

Despite simplicity and universality of Newton's law of gravity, the analytical solution of an evolving gravitational system containing just three bodies become unsolvable, let alone a complex system embracing many more objects. Thus, due to their inherently non-linear nature, the only way to study N-body dynamical problems is by means of numerical analysis.

Numerical analysis, nowadays exclusively performed by computers, consists in finding the motion of each body in the system by iteratively summing the forces on each of them over small time increments. That is, by knowing all forces acting at the beginning of a tiny time interval it becomes possible to work out the approximate position and velocity for each body of the system at its end – the so-called timestep. Proceeding in that way a very good approximate solution can always be found, just on condition of using proper numerical algorithms and small enough time increments.

The numerical analysis for this project has been applied by means of the SWIFT Solar System Dynamics code designed by Levison and Duncan (1994), running at the Centre for Astrophysics and Supercomputing at Swinburne University of Technology (Melbourne, Australia).

The SWIFT Solar System Dynamics code was developed with the main purpose to accurately integrate the orbits of small objects in the Solar System on timescales approaching its full age. Paradoxically, in order to succeed in such long-term dynamical goal the code firstly requires being able to precisely follow the short-lived close approaches between small objects and planets. Not only SWIFT fulfills both demands, but it does so very efficiently.

The SWIFT code is based on the also high efficient algorithms pioneered by Wisdom and Holman (1991), called the *Mixed Variable Symplectic* (MVS) method. In the MVS method, the Hamiltonian from which the equations of motion are derived can be written as just the sum of two independent integrable components: one representing the Keplerian motion, and the other representing the interactions – mutual perturbations of the bodies on one another. Time evolution of the system is obtained by iterating a canonical transformation – the mapping step – so that the mapping results symplectic. This guarantees that the Hamiltonian remains constant for long

integrations, or in other words, no secular changes in the energy of the system[1] (Murray & Dermott, 1999).

The improvement introduced by the SWIFT code is to treat planetary close encounters – every times a body comes in the vicinity of a planet – with particular care, as planetary perturbations can and certainly do play an important dynamical role just during such transient conditions. Physically, the region where a planet exerts higher gravitational influences than that of the Sun is called its Hill sphere, and thus it is the exclusive region for planetary perturbations. Depending on the location of the considered particle relative to a planet and its Hill radius, close encounters can or cannot take place.

Hence, in case the considered particle lies either very close to a planet – within one Hill radius – or in the "intermediate" zone – between 1 and 3.5 Hill radius – the idea is to automatically decrease the timestep of the integration with preset factors. Given that at the intermediate zone dynamical uncertainties are implicitly greater– it is the region where the forces from the Sun and the planet become comparable – the corresponding timestep decreasing factor is also higher.

Besides wisely employing different timesteps, SWIFT also takes particular advantage of the situation when a particle is located within one Hill radius of a planet. Under these circumstances, the MVS separation of the Halmitonian is performed so that the Keplerian part can be centered about the planet rather than the Sun, a treatment that allows integrating arbitrary close encounters. This improved technique is known as the *Regularized Mixed Variable Symplectic* (RMVS) method.

The SWIFT Solar System Dynamics tool can simulate up to 20 massive bodies, plus up to 1,000 massless test particles, all orbiting a single central massive object. The required dynamical parameters of each massive body or test particle can be input either by entering its six Cartesian coordinates (*x, y, z, dx/dt, dy/dt, dz/dt*) or by means of just three orbital data (eccentricity, semi-major axis, and inclination) which will be automatically converted into proper Cartesian coordinates for a random initial position. The code requires that at least two test particles are present at the beginning of the integration.

Finally, the code requires that three time parameters must be defined in advance. Two of them are of fundamental importance, as the 'total integration time' and the 'timestep' will rule the simulation; the third one, the 'data output time' – the time elapsing between each showed data – will be largely responsible for how long it will actually take. Each simulation will run for the total integration time as long as test particles remain within the system – that is, not been removed by means of either ejections or collisions.

The calculation of initial conditions

As said, this study about the capture viability of some particular satellites due to the disruption of a binary system that happened to pass close enough to the host planet is based on computational

[1] Almost all conventional direct numerical integration techniques (like the well-known Runge-Kutta method) have quadratic phase error growth caused by the linear growth of their energy errors (Gladman et al., 1991). In contrast, as symplectic integrators have no energy error growth their phase errors grow linearly, so that they become particularly suited for long-term integrations.

analysis. The model for simulating such binary-planet encounters assumes that (a) the binary system approaches the planet on a hyperbolic trajectory, and (b) the binary system can be impulsively disrupted just as a direct consequence of gravitational forces in play.

Any considered binary system following an approaching hyperbolic trajectory with respect to a steady planet can be properly characterized by a set of unique particular parameters. They can be divided into dynamical parameters, such as *speed at infinity* (v_∞) and *close approach distance* (q_e), binary orbital parameters, such as *semi-major axis* (a_{bin}), *eccentricity* (e_{bin}) and *inclination of the orbital plane* (I_{bin}), plus obviously physical parameters, such as the *masses* of each object (m_1, m_2).

In this study the binary eccentricity will always be zero ($e_{bin} = 0$) so that each member of the binary system describes a circle around the common center of mass, and also the binary orbital plane will always coincide with the plane of the hyperbolic trajectory of the common center of mass ($I_{bin} = 0$). At the same time, the mass of the first binary member (m_1) will always be equal to the mass of the moon whose case is being analyzed, and the closest approach distance of the hyperbolic trajectory will be equal to half the tidal disruption distance ($q_e = 0.5\ r_{td}$) unless otherwise explicitly stated.

The incidence of the remaining three parameters (v_∞, a_{bin}, and m_2) is the base of this present computational analysis. Each particular set of parameters defines a different physical situation, and correspondingly different consequences could be expected for each one. After a proper translation of a given parameter set into SWIFT input data, the software tool will simulate the close encounter between such incoming binary system and planet in order to dictate a computational verdict about capture viability for the binary moon candidate.

SWIFT requires knowing the exact location and velocity for each binary body at the beginning of simulation, that is, their Cartesian coordinates (x_1, y_1, z_1, dx_1/dt, dy_1/dt, dz_1/dt) and (x_2, y_2, z_2, dx_2/dt, dy_2/dt, dz_2/dt) referred to the central object (0, 0, 0, 0, 0, 0) at time t = 0. Considering that $I_{bin} = 0$, then it immediately becomes $z_1 = z_2 = dz_1/dt = dz_2/dt = 0$. The remaining coordinates can be obtained from the combination of the hyperbolic displacement of the binary's common center of mass (x_0, y_0, dx_0/dt, dy_0/dt) plus the respective circular independent movements of each body around it.

In order to facilitate the computation, the binary members are selected to be initially located at the same ordinate, which implies (a) $y_1 = y_2 = y_0$, and (b) the circular orbital velocity in the *x*-direction around the common center of mass becomes null, so that $dx_1/dt = dx_2/dt = dx_0/dt$. At the same time, $x_1 = x_0 - a_1$ and $x_2 = x_0 + a_2$, where a_1 and a_2 are respectively the radii of each one of the circular orbits, and also $dy_1/dt = dy_0/dt - v_1$ and $dy_2/dt = dy_0/dt + v_2$, where v_1 and v_2 are respectively the circular orbital speeds.

Therefore, required binary members initial conditions become known from calculating four independent binary orbital parameters (a_1, a_2, v_1, v_2), plus finding out the correspondent initial coordinates of the binary center of mass (x_0, y_0, dx_0/dt, dy_0/dt).

i) Determining the binary orbital parameters a_1, a_2, v_1, v_2.

Given m_1, m_2, and a_{bin}, the period of the binary system (P), the respective semi-major axes (a_1, a_2) of the orbits around the common center of mass – which in this case actually are radii – and their respective circular speeds (v_1, v_2), become determined according to the following formulas:

$$P = \sqrt{\frac{4\pi^2 a_{bin}^3}{G(m_1 + m_2)}} \qquad \{8\}$$

$$a_1 = \frac{m_2}{m_1 + m_2} a_{bin} \quad \text{and} \quad a_2 = \frac{m_1}{m_1 + m_2} a_{bin} \qquad \{9\}$$

$$v_1 = \frac{2\pi a_1}{P} \quad \text{and} \quad v_2 = \frac{2\pi a_2}{P} \qquad \{10\}$$

where G is the universal gravitational constant.

ii) Converting dynamical parameters of the hyperbolic trajectory into planetocentric Cartesian coordinates (x_0, y_0, dx_0/dt, dy_0/dt)

The two geometrical parameters that define a coplanar hyperbolic curve are its semi-major axis (a_h) and eccentricity (e_h), so called by extension of the properties for the ellipse case, and then generically applied for any conic-section derived curve. Hence, the distance from the focus to a given point on the hyperbola (r) that lays at an angle (φ) from the symmetrical axis that cuts the curve is

$$r = \frac{a_h(e_h^2 - 1)}{1 - e_h \cos\varphi} \qquad \{11\}$$

The closest distance to the focus (q_e) results when φ = 180°, thus becoming

$$q_e = a_h(e_h - 1) \qquad \{12\}$$

The speed (v_h) of a moving object in a hyperbolic trajectory due to the only gravitational influence of a steady body placed at its focus, results

$$v_h = \sqrt{G(M + m)\left(2/r + 1/a_h\right)} \qquad \{13\}$$

where m is the mass of the moving object (or $m = m_1 + m_2$ for an approaching binary system), and M is the mass of the steady body. Therefore, at infinity (where $r = \infty$) velocity results

$$v_\infty = \sqrt{\frac{G(M + m)}{a_h}} \qquad \{14\}$$

From equations {12} and {14} it results that the dynamical parameters v_∞ and q_e define unequivocally the geometrical coefficients a_h and e_h, and vice versa.

As already explained, the tidal disruption distance becomes equal to

$$r_{td} = a_{bin}\left(\frac{3M_P}{m_1+m_2}\right)^{1/3} = R_P\left(\frac{a_{bin}}{R_1}\right)\left[\left(\frac{3\rho_P}{\rho_1}\right)\left(\frac{m_1}{m_1+m_2}\right)\right]^{1/3} \qquad \{15\}$$

where a_{bin} is the binary semi-major axis, M_P, R_P, ρ_P are respectively the mass, radius, and density of the planet, as well as m_1, R_1, ρ_1 represent the same for the larger binary member, while m_2 is the mass of the smaller one. Considering object #1 to be the potential candidate for becoming captured, m_1 and ρ_1 have to be equal to actual physical values of the satellite in question and thus both known, as well as R_P.

The closest distance to the focus (q_e) is chosen to be 0.5 r_{td}, so that from equation {15} such distance becomes known for any given values of parameters a_{bin}/R_1 and m_2. Consequently, based on the assumptions already taken, the hyperbolic curve to be described and the velocity at any point become perfectly determined once arbitrary values for a_{bin}, m_2, and v_∞ are given.

The greatest velocity of the binary common center of mass following the hyperbolic trajectory takes place at its closest distance to the planet (v_q), and then it can be found by replacing r by q_e in equation {13}. The position of the binary center of mass on the hyperbolic trajectory at the beginning of each simulation (r_0) has to be wisely selected: not too far from the planet so that to avoid wasting unproductive integration time, not too close from the planet so that to avoid provoking immediate binary disruption. The arbitrary chosen criterion – whose properness was later on effectively corroborated – is to start all simulations from the instant when the binary center of mass lays at a distance to the planet equal to maximum orbital speed times the binary period, thus $r_0 = v_q \times P$.

Having r_0, the corresponding initial angle φ_0 can be derived from equation {11}, and hence the coordinates of the common center of mass simply become

$$x_0 = r_0 \cos\varphi_0 \qquad \{16\}$$

$$y_0 = r_0 \sin\varphi_0 \qquad \{17\}$$

and correspondent velocity coordinates result

$$\frac{dx_0}{dt} = -\sqrt{\frac{G(M_P+m_1+m_2)}{a_h(e_h^2-1)}}\sin\varphi_0 \qquad \{18\}$$

$$\frac{dy_0}{dt} = \sqrt{\frac{G(M_P+m_1+m_2)}{a_h(e_h^2-1)}}(\cos\varphi_0 - e_h) \qquad \{19\}$$

where M_P represents the mass of the central planet (Murray & Dermott, 1999).

Description of the experiments

In order to investigate the viability of the model for satellite capture by binary-planet encounters three practical cases have been analyzed: Neptune's largest moon (Triton), and the two small Martian moons (Phobos and Deimos). These cases were selected as a genuine challenge for the model under test, given not only the wide intrinsic difference in satellite masses, but of Hill spheres of host planets as well. On the one hand, Triton has a huge mass and moves around its large parent planet on a very inclined and retrograde orbit; on the other hand, both Phobos and Deimos appear as 'regular' tiny Martian satellites, although there is general agreement that they were also captured (S. Fred Singer, 2003).

Triton's likely capture due to a binary-planet encounter had been firstly analyzed by Agnor & Hamilton (2006). About the potential capture of the Martian moons by means of the binary-planet encounter mechanism, so far no published literature could be found.

Despite the origin of incoming binary systems for each case necessarily has to be different (from the Kuiper Belt for Neptune, from the asteroid belt for Mars), dynamically is still the same issue. In consequence, runnings for Triton's, Phobos' and Deimos' cases only differed in the numeric values for the masses of corresponding planet, satellite-candidate and companion.

All simulations were performed embracing exclusively the three bodies in question – the binary system and the planet – a much simpler but still valid scenario for this study than including other massive distant objects. In any case, several simulations were actually performed positioning the Sun as the central object, but they proved to be highly time-consuming (passing from a planetocentric to an equivalent heliocentric simulation requires larger integration times) and worthless (outcomes from long heliocentric simulations were basically the same from short planetocentric ones, except for the omission of the ulterior predictive solar gravitational effect).

For each simulation, time parameters were selected according to the following criteria:

1) The total integration time was arbitrarily chosen as 25 times the period of the binary system (as it took 3 or 4 periods for the binary system to reach q_e, simulations still lasted for a proper interval in order to show stabilized results).
2) The timestep was initially chosen following the thumb rule as 1/20 of the considered period (which generally assures the right balance between precision and time investment). However, in a few cases where obtained outcomes achieved larger values for resulting $a_{1,2}$ or $e_{1,2}$ (as a direct consequence of numerical unstabilities) in order to obtain coherent and trustful results it was necessary to rerun those simulations with new timesteps as low as 1/100 of their previous values.
3) The output data time was always defined as 1/2000 the total integration time (that is, the maximum allowed value).

For each simulation it was recorded the final semi-major axis (a_1 and a_2) and eccentricity (e_1 and e_2) of each object of the incoming binary system. Much more than 500 simulations were performed along this study, consuming about 40 hours of processing time (~ 5 minutes each).

The simulation of Triton's capture

The selection of the ranges of input parameters (v_∞, a_{bin}, and m_2) was made taking into account Agnor & Hamilton's experience, but trying to diversify them in order to analyze a broad scenario. In consequence, the range for v_∞ was defined to vary from 100 to 3,200 m/s (higher values are very unlikely, as passing-by binary KBOs have slow speeds relative to Neptune, even for Centaurs[2]); the range for a_{bin} was from 4 to 500 Triton's radius (larger semi-major axes for a binary KBOs seem improbable), while the range for m_2 was from 0.05 to 1.35 Triton's mass (larger relative mass differences for KBOs also seem not very probable).

Regarding that for a potential capture v_∞ becomes the parameter of major incidence, its full range was then divided into six values (100, 200, 400, 800, 1600, and 3200 m/s, each value doubling the previous one), while for the other two parameters a_{bin}, and m_2 only four were allowed (for a_{bin}: 4, 20, 100, and 500 Triton's radius, for m_2: 0.05, 0.15, 0.45, and 1.35 Triton's mass, each value respectively 5 and 3 times larger than previous ones). That makes 96 possible combinations. For each one possible combination of input parameters, one simulation was performed.

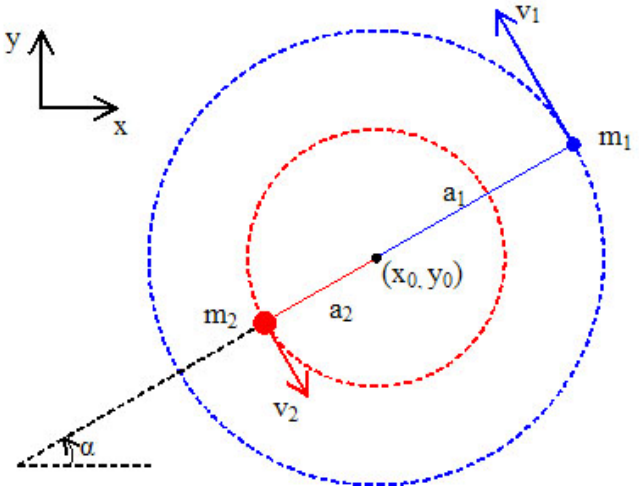

$$x_1 = x_0 + a_1 \cos\alpha$$
$$y_1 = y_0 + a_1 \sin\alpha$$
$$x_2 = x_0 - a_2 \cos\alpha$$
$$y_2 = y_0 - a_2 \sin\alpha$$
$$v_{1x} = v_{0x} - v_1 \sin\alpha$$
$$v_{1y} = v_{0y} + v_1 \cos\alpha$$
$$v_{2x} = v_{0x} + v_2 \sin\alpha$$
$$v_{2y} = v_{0y} - v_2 \cos\alpha$$

Figure 1
The orbital phase analysis
At right appear the expressions for the Cartesian coordinates for position and velocity for each binary member, depending on the angle between the line joining them and the x-axis.

With the specific objective to analyze the incidence of the relative orbital initial positions of each binary member – the orbital phase – series of 12 simulations were performed for exactly the same v_∞, a_{bin}, and m_2 parameters, just each time varying 30 degrees counterclockwise the relative initial location of binary members. The relations for obtaining the corresponding Cartesian coordinates for both position and velocity are shown in Figure 1.(In such context, all "regular" simulations were performed for α = 180°).

---

[2] Relative to Neptune, crossing objects achieve $v_\infty \approx e_H v_N$ (Agnor & Hamilton, 2006) where e_H is the heliocentric eccentricity of the object, and v_N is Neptune's orbital speed. Centaurs are KBOs with highly unstable orbits which usually have high eccentricities – so that they usually are crossing Neptune's orbit. In particular a binary Centaur (2002 CR_{46}) has been already found (Selby Cull, 2006).

Two cases were selected for testing orbital phase incidence: one corresponding to a case that had been originally cataloged as a 'strong' positive-capture case (v_∞ = 800 m/s, m_2 = 1.35 M_{Trit}, a_{bin} = 20 R_{Trit}, giving a = 0.024 AU, e = 0.941 and still a permanent capture even if one parameter were changed to its next tried value), while the other corresponding to a 'non-capturing' case (v_∞ = 400 m/s, m_2 = 0.45 M_{Trit}, a_{bin} = 100 R_{Trit}, giving a = 1.131 AU, e = 0.992) that at least resulted a transitory capture.

The simulation of Phobos' capture

The selection of input parameter ranges for this second case was made after several tentative runnings were performed. Clearly, the tiny mass of the red planet greatly restrains its capturing potential (in this case, even the lowest v_∞ tried for Triton's case provoked too high kinetic energies). In consequence, the range for v_∞ was defined to vary from 0.1 to 100 m/s (that is, starting from a very unlikely small value up to a respectable one; higher values for potential crossing binary objects, although possible, will certainly not result in captures according to several actually performed simulations); the range for a_{bin} was from 4 to 500 Phobos' radius (which seems to fairly cover the expected semi-major axis length for binary asteroids), while the range for m_2 was from 0.1 to 100 Phobos' mass (which seems to properly cover all relative mass spectrum for binary asteroids).

As same as for previous case, the full range for v_∞ was then divided into six values (0.1, 0.4, 1.6, 6.4, 25, and 100 m/s, each value about 4 times larger than the previous one), 4 values for a_{bin} (4, 20, 100, and 500 Phobos' radius, each value 5 times greater) and also 4 values for m_2 (0.1, 1, 10, and 100 Phobos' mass, each value one order of magnitude greater), also making 96 possible combinations.

Given the obtained capture results, another 96 simulations were run for the same input parameters, but this time imposing to the closest distance to the focus (q_e) of the incoming hyperbolic trajectory of the binary center of mass to be just 0.1 of the tidal disruption distance (r_{td}), that is, to become five times closer to the planet than before, when $q_e = 0.5\ r_{td}$.

Finally, two cases were also selected for testing orbital phase incidence (v_∞ = 6.4 m/s, m_2 = 10 M_{Phob}, a_{bin} = 20 R_{Phob} and v_∞ = 100 m/s, m_2 = 100 M_{Phob}, a_{bin} = 20 R_{Phob}). They were selected because results were relative close to positive-cases (respectively, a = 0.05 AU, e = 0.998 for the first one, and a = 0.012 AU, e = 1.008 for the second).

The simulation of Deimos' capture

The selection of input parameter ranges for Deimos' case was made equal than for Phobos'. In consequence, six values were chosen for v_∞ (0.1, 0.4, 1.6, 6.4, 25, and 100 m/s), 4 values for a_{bin} (4, 20, 100, and 500 Deimos' radius), and also 4 values for m_2 (0.1, 1, 10, and 100 Deimos' mass), thus also making 96 possible combinations.

Not specific orbital phase study was performed, but the fact that there was a case having $m_2 = 1 = m_1$ implied that capture analysis was simultaneously done for both objects (as if it were two phases of the same case).

Results and Discussion

For the three particular cases considered, simulations always ended with the incoming binary system disrupted, each object achieving an independent trajectory after close interaction with the planet took place. This was an expected outcome, as all hyperbolic curves were forced to pass very close to planets (at least at half the corresponding tidal disruption distance).

Also, as it should be, no single simulation ended with eccentricity for both objects lesser than 1 (the gravitational interaction with the planet can rearrange orbital energy of binary members and it certainly does, but the rise of one body is done at the expense of the other's fall). Therefore, results from simulations were of only two possible types after disruption took place: either (i) one eccentricity greater than 1, while the other lesser than 1, or (ii) both eccentricities greater than 1. The first type corresponded to one object becoming transitory captured (as Figure 2 shows al left), while the second type corresponded to both objects flying away per independent curves (too much initial kinetic energy, as Figure 2 exemplifies at right).

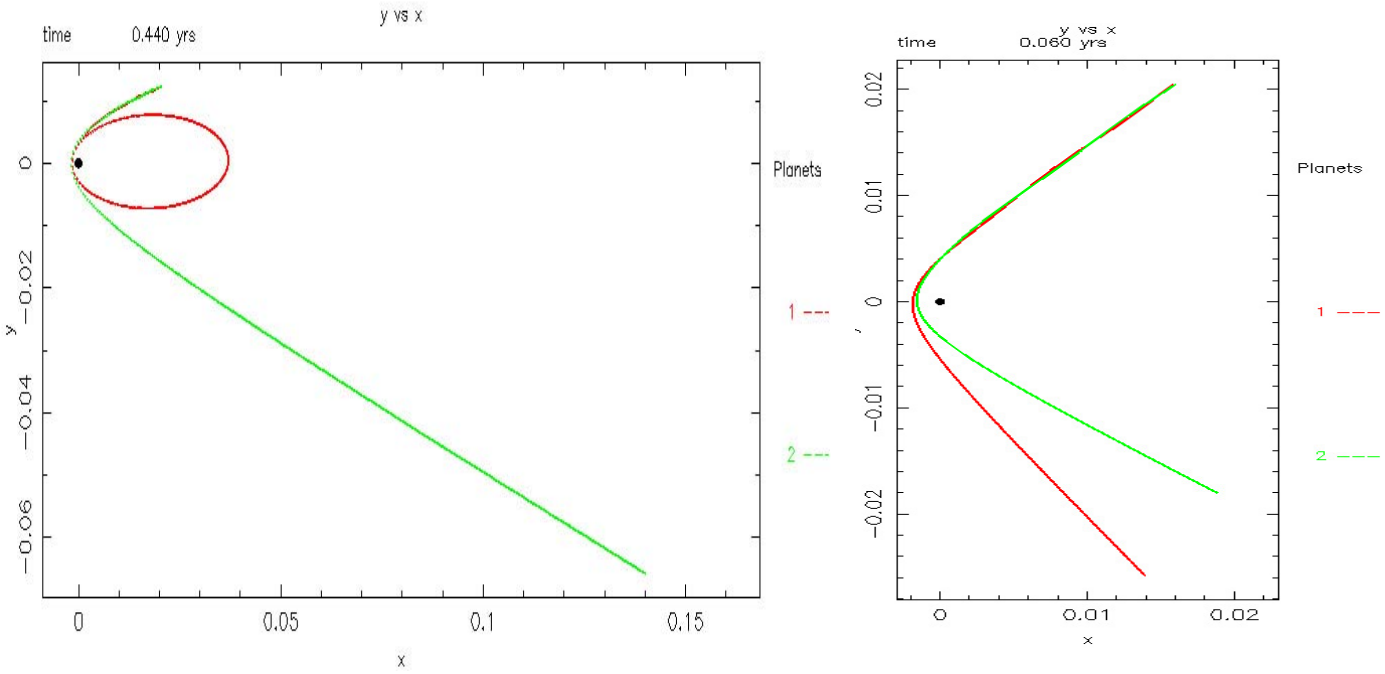

Figure 2
Typical y vs x plots from simulations mimicking binary-planet encounters.
At left, the case where object # 1 becomes captured; at right, both members escape after disruption.
Parameters corresponding to each graph are detailed in the next related figures.

Figure 3 presents eccentricity versus time for the binary-planet encounter shown at left in Figure 2. Initially, each binary object orbits around the common center of mass, so from the planetocentric view, both eccentricities oscillate – with the binary period – around a common fixed value (in this case, slightly greater than 1). As the binary system approaches the planet each member experiments here increasingly gravitational influences (clearly denoted by the strong increase of the envelope of relative maximums of each eccentricity curves) until the binary system becomes definitively disrupted (occurring for $t \approx 0.04$ years). Afterwards, in this example, object # 1 becomes captured ($e_1 \approx 0.92$), while object # 2 escapes ($e_2 \approx 1.07$).

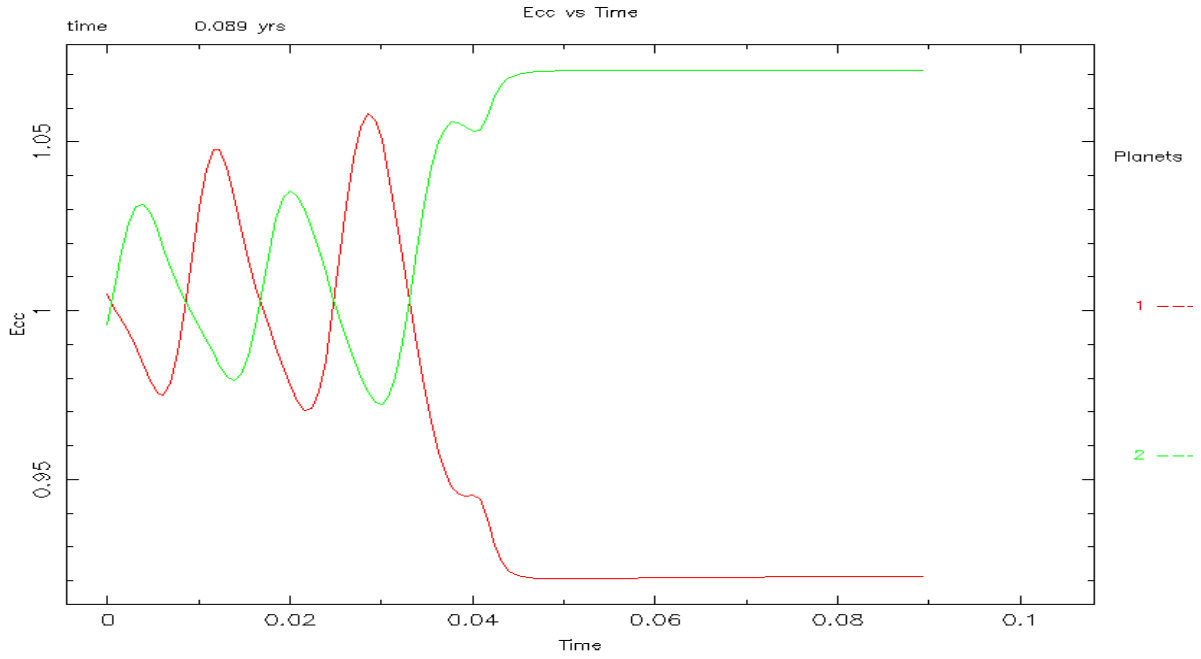

Figure 3
Typical eccentricity vs time plot for a binary-planet encounter, where the object # 1 becomes captured after disruption (for t = 0.04 yr). Triton's case simulation: = 200 m/s, m_2 = 1.35 M_{Trit}, a_{bin} = 20 R_{Trit}.

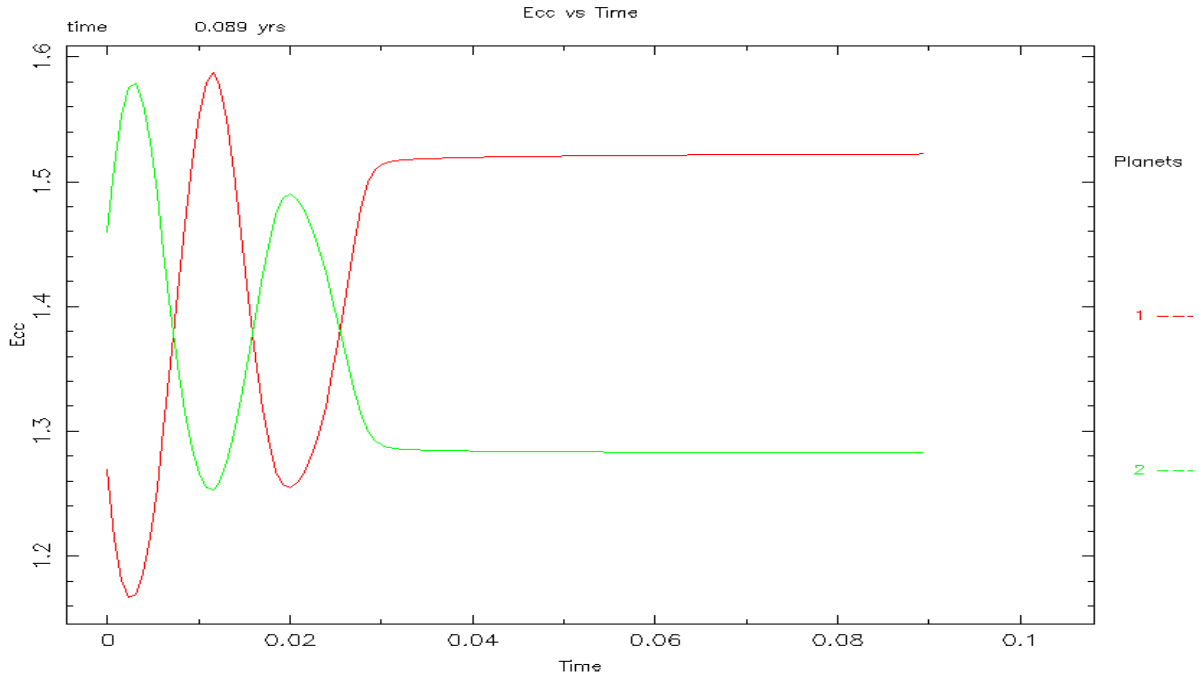

Figure 4
Typical eccentricity vs time plot for a binary-planet encounter, where none of the objects become captured after disruption (for t 0.03 yr). Triton's case simulation: = 3200 m/s, m_2 = 1.35 M_{Trit}, a_{bin} = 20 R_{Trit}.

Figure 4 presents eccentricity versus time for the binary-planet encounter shown at right in Figure 2, where dynamical results are totally different. Here, previous to disruption (occurring for $t \approx 0.03$ years), both "incoming" eccentricities oscillate while decreasing their relative maximums around $e \approx 1.37$ (an "excessive" kinetic energy for permitting a capture). In this case, both object rapidly escapes ($e_1 \approx 1.52$, $e_2 \approx 1.29$) after the encounter took place.

As said before, $e_1 < 1$ only implies a transitory capture of the satellite candidate. According to equation {7} permanent captures for Triton's case are only possible on condition that corresponding $a_1 < 0.388$ AU, while for Martian's moons it is required $a_1 < 0.0036$ AU (less than one hundredth the previous value).

Triton's case

Results for the performed 96 simulations appear in the following page, as well as corresponding input v_∞, a_{bin}, and m_2 parameters for each run. In yellow appear 37 results that simultaneously verify $a_1 < 0.388$ AU and $e_1 < 1$, that is, there were found 37 cases of binary-Neptune encounters ending in permanent ('positive') capture of an object with the same mass as Triton. It becomes worth mentioning that the eccentricity for all positive-cases was always pretty high ($e \geq 0.918$).

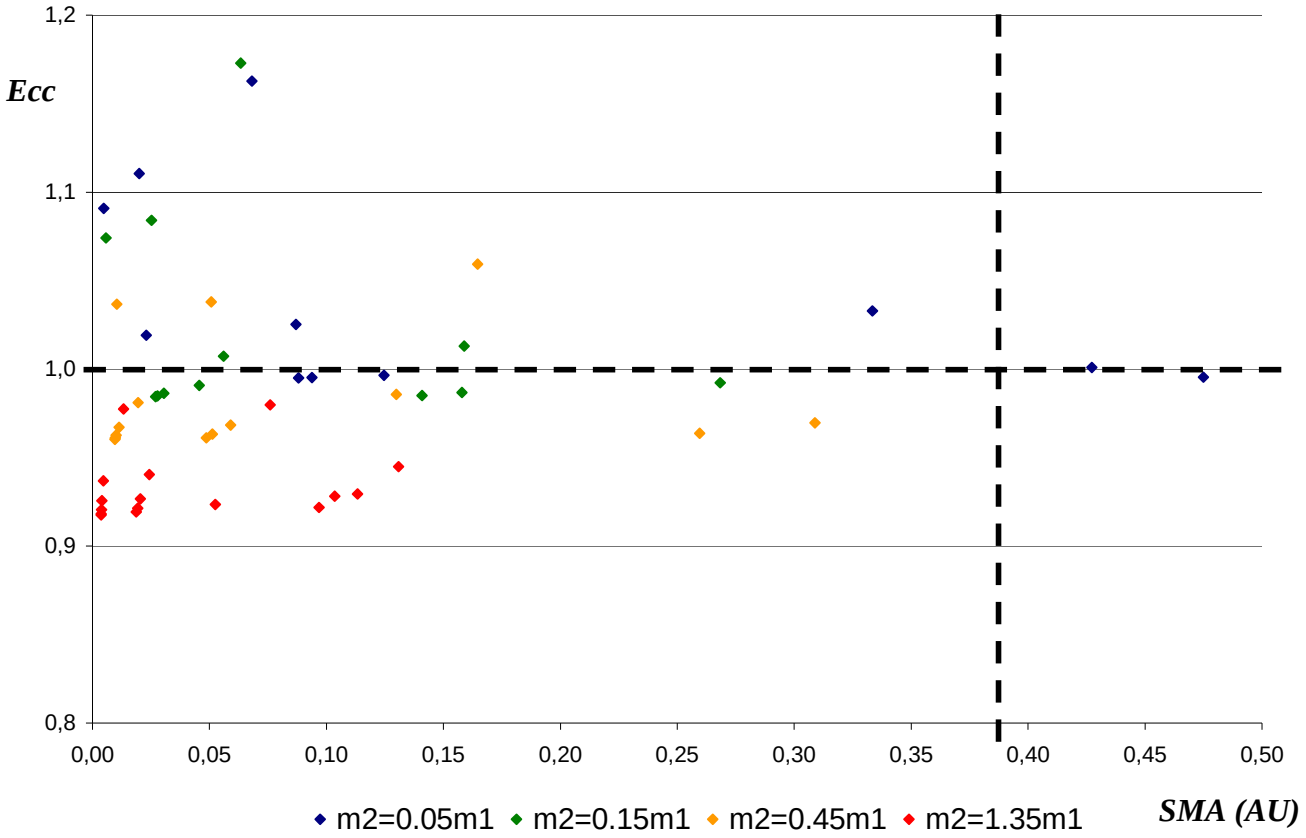

Figure 5
Final eccentricity vs final semi-major axis (in AU) of the Triton-candidate object after binary disruption. The graph only shows those results obtained where SMA are smaller than 0.5 AU, and eccentricities lower than 1.2. Different colours are used to represent results obtained for different masses of the binary companion, for 24 different combinations of velocity at infinity and binary SMA parameters.

v(inf) (m/s)	a_bin (RTrit)	m2 (mTrit)	SMA #1	ecc #1
100	4	0,05	0,0881	0,9950
200	4	0,05	0,0938	0,9953
400	4	0,05	0,1246	0,9965
800	4	0,05	0,4272	1,0010
1600	4	0,05	0,0229	1,0191
3200	4	0,05	0,0048	1,0909
100	20	0,05	0,4749	0,9954
200	20	0,05	0,6972	0,9969
400	20	0,05	0,8639	1,0025
800	20	0,05	0,0869	1,0252
1600	20	0,05	0,0199	1,1106
3200	20	0,05	0,0043	1,5094
100	100	0,05	4,0881	0,9973
200	100	0,05	2,4725	1,0044
400	100	0,05	0,3334	1,0328
800	100	0,05	0,0682	1,1628
1600	100	0,05	0,0179	1,8283
3200	100	0,05	0,0045	3,4306
100	500	0,05	8,0823	1,0068
200	500	0,05	1,2918	1,0423
400	500	0,05	0,2752	1,2019
800	500	0,05	0,0719	1,7605
1600	500	0,05	0,0195	9,3268

v(inf) (m/s)	a_bin (RTrit)	m2 (mTrit)	SMA #1	ecc #1
100	4	0,15	0,0270	0,9845
200	4	0,15	0,0277	0,9849
400	4	0,15	0,0305	0,9863
800	4	0,15	0,0456	0,9908
1600	4	0,15	0,0560	1,0074
3200	4	0,15	0,0057	1,0741
100	20	0,15	0,1408	0,9851
200	20	0,15	0,1580	0,9867
400	20	0,15	0,2684	0,9922
800	20	0,15	0,1589	1,0131
1600	20	0,15	0,0252	1,0840
3200	20	0,15	0,0042	1,5156
100	100	0,15	0,8277	0,9873
200	100	0,15	1,7081	0,9939
400	100	0,15	0,5130	1,0203
800	100	0,15	0,0633	1,1730
1600	100	0,15	0,0180	1,5817
3200	100	0,15	0,0045	3,3706
100	500	0,15	1,6985	0,9693
200	500	0,15	1,7821	1,0292
400	500	0,15	0,2597	1,2104
800	500	0,15	0,0728	1,7109
1600	500	0,15	0,0179	4,1189

v(inf) (m/s)	a_bin (RTrit)	m2 (mTrit)	SMA #1	ecc #1
100	4	0,45	0,0095	0,9603
200	4	0,45	0,0097	0,9612
400	4	0,45	0,0101	0,9626
800	4	0,45	0,0114	0,9671
1600	4	0,45	0,0194	0,9810
3200	4	0,45	0,0103	1,0368
100	20	0,45	0,0486	0,9612
200	20	0,45	0,0512	0,9632
400	20	0,45	0,0590	0,9683
800	20	0,45	0,1298	0,9858
1600	20	0,45	0,0507	1,0379
3200	20	0,45	0,0039	1,5178
100	100	0,45	0,2596	0,9637
200	100	0,45	0,3088	0,9697
400	100	0,45	1,1306	0,9918
800	100	0,45	0,1647	1,0594
1600	100	0,45	0,0156	1,6490
3200	100	0,45	0,0045	3,0521
100	500	0,45	1,6311	0,9715
200	500	0,45	11,2990	0,9989
400	500	0,45	0,2263	1,2301
800	500	0,45	0,0766	1,6087
1600	500	0,45	0,0180	3,4383

v(inf) (m/s)	a_bin (RTrit)	m2 (mTrit)	SMA #1	ecc #1
100	4	1,35	0,0037	0,9176
200	4	1,35	0,0037	0,9183
400	4	1,35	0,0038	0,9205
800	4	1,35	0,0040	0,9256
1600	4	1,35	0,0046	0,9369
3200	4	1,35	0,0132	0,9774
100	20	1,35	0,0187	0,9192
200	20	1,35	0,0193	0,9215
400	20	1,35	0,0204	0,9268
800	20	1,35	0,0243	0,9405
1600	20	1,35	0,0760	0,9797
3200	20	1,35	0,0035	1,5334
100	100	1,35	0,0968	0,9219
200	100	1,35	0,1036	0,9281
400	100	1,35	0,1309	0,9450
800	100	1,35	0,1132	0,9294
1600	100	1,35	0,0145	1,6286
3200	100	1,35	0,0047	2,5993
100	500	1,35	0,5262	0,9296
200	500	1,35	0,7292	0,9507
400	500	1,35	0,0525	0,9236
800	500	1,35	0,0513	1,8676
1600	500	1,35	0,0186	2,9484

Just from a rapid inspection of the relative position that positive cases occupy in the tables it results that positive cases seems to be favoured by larger mass of Triton-candidate companion, by smaller velocity at infinity, and also by smaller binary orbits.

Figure 5 partially plots the final eccentricity versus final semi-major axis of object # 1 obtained from the 96 simulations, showing only those results with lowest eccentricities and SMAs. Points of same colour represent outcomes obtained from simulations ran for the same mass of the companion object. The vertical dashed line corresponds to 0.388 AU, so that the 37 coloured points lying at its left and under $e = 1$ actually represent the positive capture cases.

A more detailed and objective analysis for Triton's case can be done based on comparison of data extracted from the following graphs.

Final eccentricity of the Triton-candidate object after binary disruption

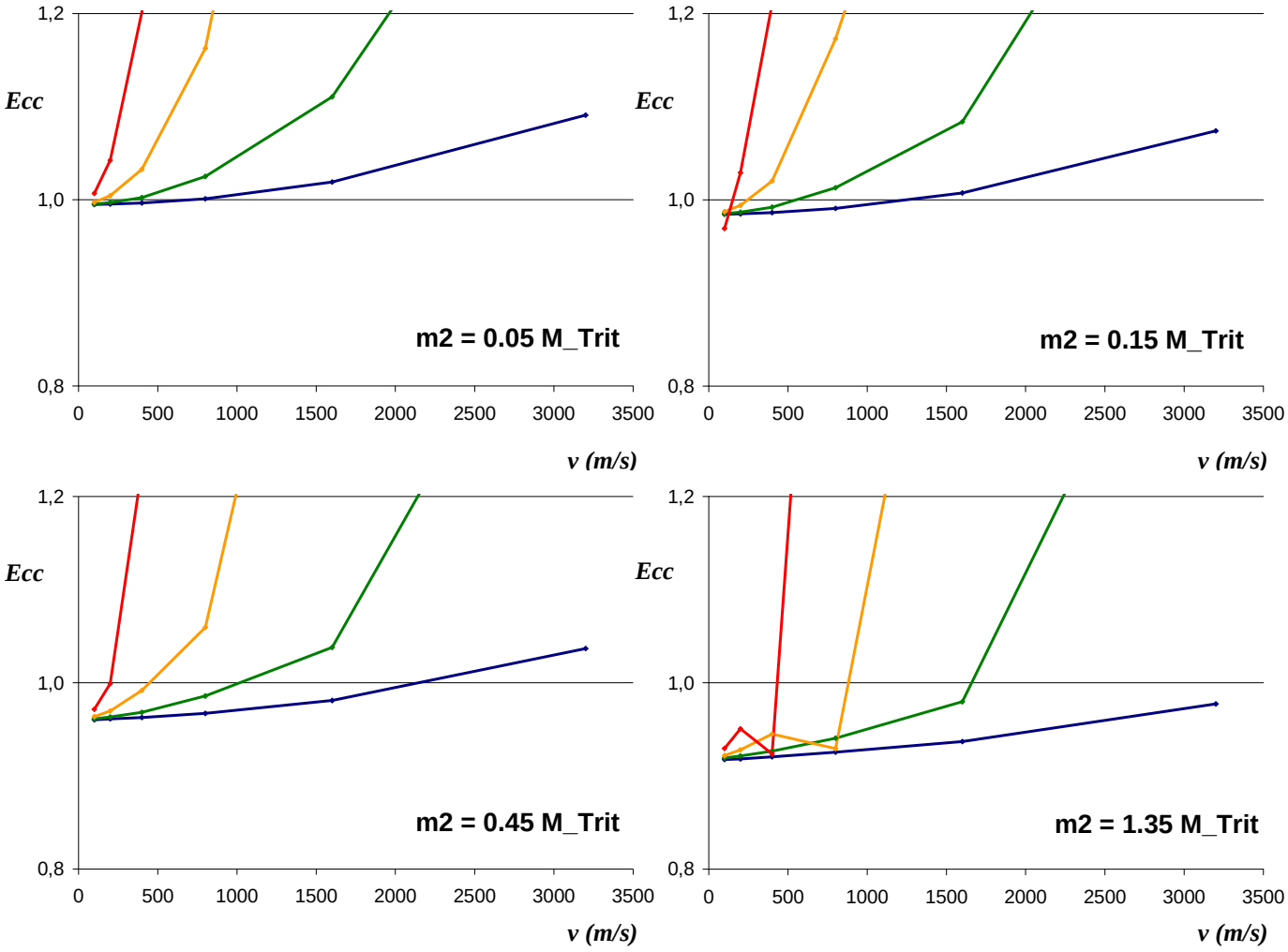

Figure 6
Final eccentricity of object # 1versus velocity at infinity (m/s) of the incoming binary system. Each one of the cases for stated mass of object # 2. All cases compare the relative incidence of the a_{bin} factor (blue lines are used for 4 AU, while green for 20 AU, orange for 100 AU, and red for 500 AU).

Figure 6 compares final eccentricity of object # 1 versus the full considered range for velocity at infinity, as it varies the semi-major axis of the binary system, and for a given mass of the binary companion. As the graphs clearly show, in order to achieve potential captures ($e_1 < 1$):

1) The lower v_∞, the better (lower v_∞ means smaller overall kinetic energies for both incoming binary members, so that increasing capture chances).
2) The greater m_2, the better (according to equation {5}, a more massive companion makes the satellite candidate to achieve larger orbital speeds, which in turn facilitates to achieve temporarily higher drops in its net velocity referred to the planet). Just by comparing the graphs it immediately results that, given the same v_∞ and a_{bin}, lower e_1 are obtained from greater m_2.
3) The lower a_{bin}, the better (for any given binary companion, the nearer its distance, the greater the orbital speed of the satellite candidate – equation {5} – thus also helping to provoke the same effect as the previous point).

The analysis of the incidence of the orbital phase was performed for two particular Triton's cases, one corresponding to an original 'capture' case ($e_1 = 0.94$, $a_1 = 0.024$ AU) corresponding to parameters $v_\infty = 800$ m/s, $a_{bin} = 20\ R_{Trit}$, $m_2 = 1.35\ M_{Trit}$ (Figure 7), while the other to an original 'non-capture' case ($e_1 = 0.99$, $a_1 = 1.105$ AU) corresponding to parameters $v_\infty = 400$ m/s, $a_{bin} = 100\ R_{Trit}$, $m_2 = 0.45\ M_{Trit}$ (Figure 8).

From the orbital phase studies, it can be concluded the following:

1) Effectively, the relative orbital position of the binary members does affect the succeeding dynamical state that each object achieves after the binary system becomes disrupted.
2) For the considered cases, the shape of the final eccentricity curves (shown in dashed lines) is practically very similar, while the shape of the final semi-major axes changes dramatically.
3) Qualitatively, eccentricity curves have mirror-symmetry with respect to each other, surely affected by relative mass differences.
4) Quantitatively, phase variation in final eccentricity of the moon candidate (object # 1) in the first case is slightly higher than in the second case, while phase variation in final eccentricity of companion (object # 2) is slightly lower in the first case compared to the second. These results are originated in the fact that in the first case $m_1 < m_2$, so that object # 1 experiences a major change in velocity than object # 2, and vice versa for the second case.
5) For both cases, the best capturing condition (lower possible values for e_1 and a_1 at the same time) occurs for $\alpha \approx 60°$.
6) There are two zones (around $\alpha \approx 45°$ and $\alpha \approx 215°$) where minor angle changes result in major variations in the resulting eccentricity.
7) The orbital phase position actually selected for performing all Triton's simulations ($\alpha = 180°$) lays within eccentricity "stabilized zone" for both cases, while at the same time corresponds to the worst capture condition for the second case, as a_1 achieves its maximum value).
8) For both cases, both objects achieve eccentricity lesser than unity for half the full angular range. For the first case, where $a_1 < 0.388$ AU always, this means captures are viable for half the possibilities (180° out of 360°).
9) The second case also exhibits $e_1 < 1$ from about 48° to 218°, but in that region $a_1 < 0.388$ AU only from 48° to 78°. Therefore, this case that originally was cataloged as 'non-capture' due to its high a_1, actually still has a positive capture probability of 8.3 % (30° out of 360°).

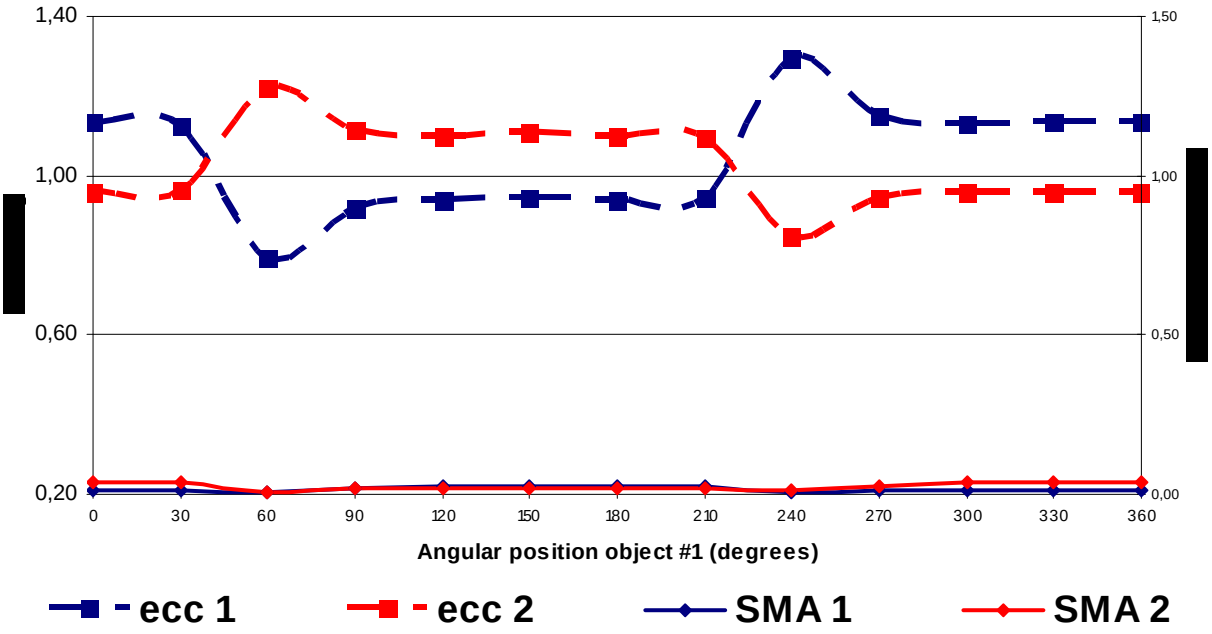

Figure 7
The orbital phase study for a 'capture' case (= 800 m/s, a_{bin} = 20 R_{Trit}, m_2 = 1.35 M_{Trit})
The graph shows the final eccentricity and semi-major values obtained from 12 simulations, each one started by rotating 30 degrees the initial position of binary object # 1 with respect to the x-axis.

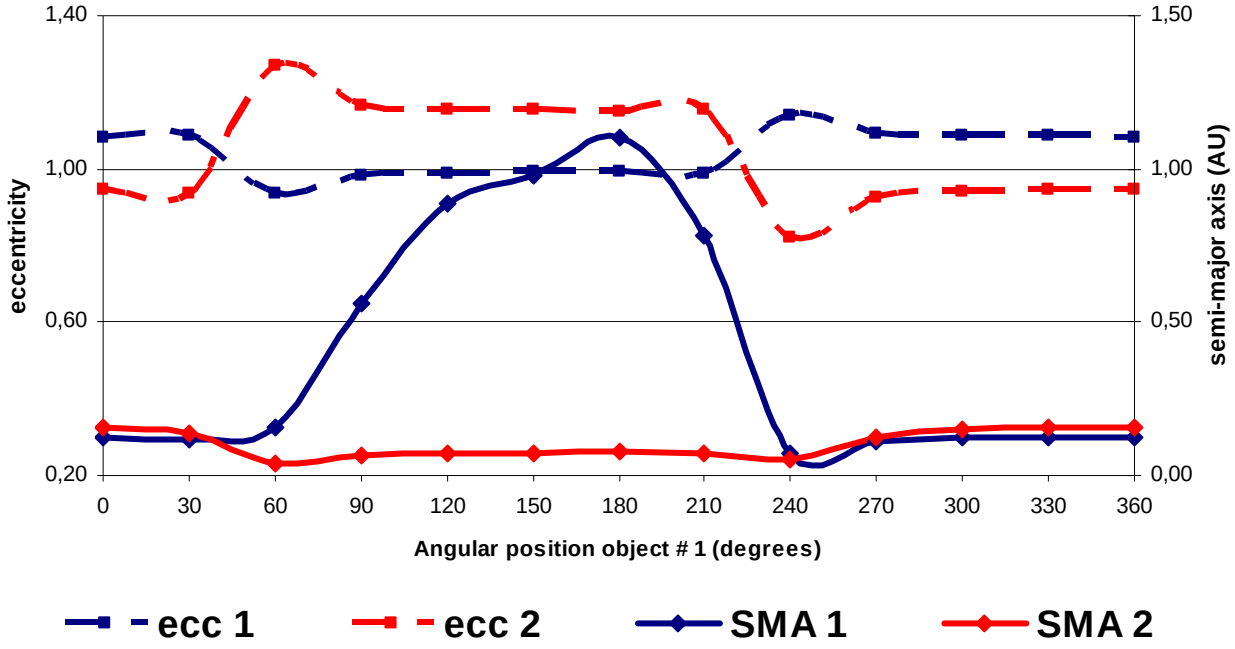

Figure 8
The orbital phase study for a 'non-capture' case (= 400 m/s, a_{bin} = 100 R_{Trit}, m_2 = 0.45 M_{Trit})
The graph shows the final eccentricity and semi-major values obtained from 12 simulations, each one started by rotating 30 degrees the initial position of binary object # 1 with respect to the x-axis.

Extrapolating conclusions obtained from the partial phase orbital analysis to the rest of the 96 individual performed simulations, it could be inferred that:

a) Due to a close binary-planet encounter, the capture by Neptune of a Triton-like object from a binary system appears totally plausibly;
b) Such captures would occur with a probability up to 50% for 'favourable' combinations of v_∞, a_{bin}, and m_2 parameters (the same conclusion obtained by Agnor & Hamilton in 2006);
c) The 37 positive-capture cases found in this work belong to such category of 'favourable' parameter combinations for satellite capture;
d) Other than those 'favourable' cases, there are many more combinations of v_∞, a_{bin}, and m_2 parameters that also allow a follow-up capture, although with (much) lower probabilities of success;
e) Considered each parameter isolated, captures are still potentially possible for (i) any value for the velocity at infinity that real binary KBO systems approaching Neptune can achieve (from almost null up to as high as 3,500 m/s, as already mentioned, the highest expected for binary Centaurs crossing Neptune's orbit), (ii) almost any companion mass (from as low as 0.05 M_{Trit} up to no upper limit, as larger companion masses clearly favour captures according to equation {5}), and (iii) almost any binary semi-major axis (from no minimum up to 500 R_{Trit}, a more than respectable large value for binary KBO systems).

Phobos' case

Figure 9 presents the final eccentricity versus final semi-major axis for binary object # 1 obtained from the performed 96 simulations, although only showing those results with lowest eccentricities and SMAs. Considering that a Phobos-like object can be permanent captured whenever $e < 1$ and at the same time $a < 0.0036$ AU, clearly not even a single positive case has resulted.

In order to facilitate capturing conditions, another 96 simulations were run for the same input parameters, but this time forcing the hyperbolic trajectory to pass closer to Mars (thus using a new $q_e = 0.1\ r_{td}$ instead of the 5 times greater previous value). Corresponding new results appear plotted in Figure 10, in just the same conditions of Figure 9.

In this new context, three positive cases were found, although very close to frontier lines. Actually, one of them ($a = 0.0037$, $e = 0.8856$) is slight outside, while the other two have eccentricity ≈ 1 ($a = 0.0030$, $e = 0.9947$, and $a = 0.0031$, $e = 0.9949$), corresponding to parameters $v_\infty = 1.6$ m/s, $a_{bin} = 100\ R_{Phob}$, $m_2 = 100\ M_{Phob}$ for the first one; $v_\infty = 0.1$ m/s, $a_{bin} = 4\ R_{Phob}$, $m_2 = 100\ M_{Phob}$ for the second; and $v_\infty = 25$ m/s, $a_{bin} = 4\ R_{Phob}$, $m_2 = 100\ M_{Phob}$ for the last.

Comparing Figures 9 and 10, it can be inferred that the new closer passage of the binary system does provoke much more cases of low eccentricity and semi-major axis for the Phobos-like object than before, although such results are still far for expecting possible captures.

Predictably, the phase analysis performed for two cases did not show any capture-privileged angular position that would have resulted hidden from previous analysis. Figures 11 and 12 depict the respective curves. Anyway, an interesting abrupt decrease both in eccentricity and SMA was found for a narrow zone around $\alpha \approx 60°$, although still $a > 0.0036$ AU.

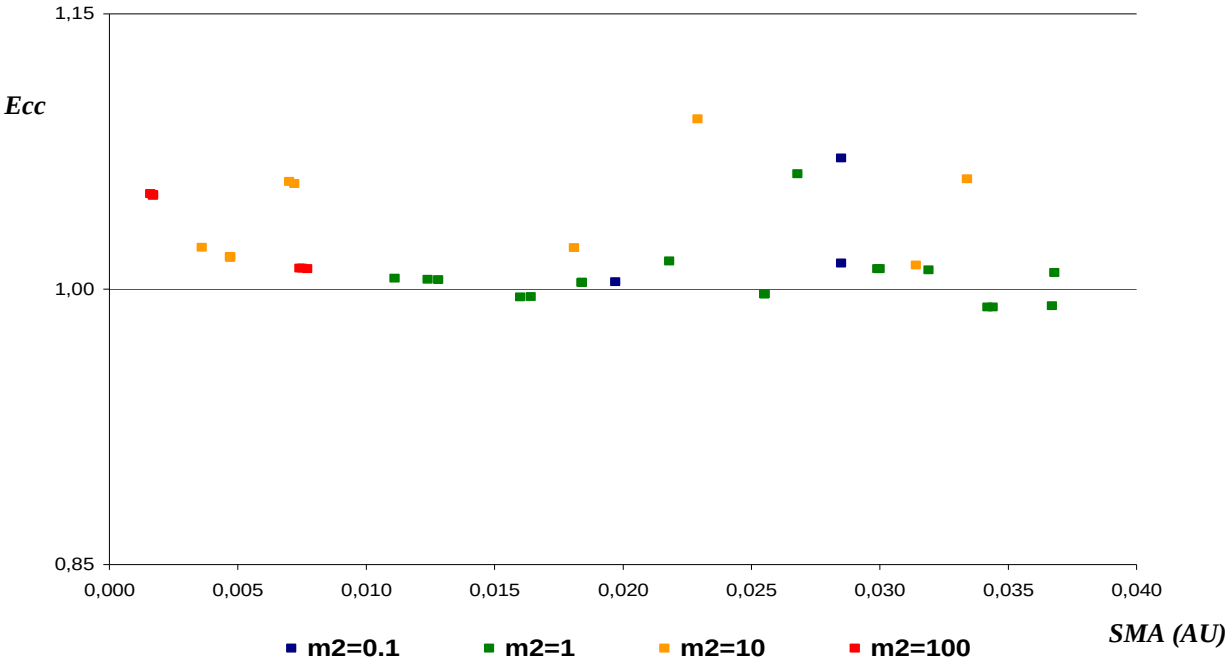

Figure 9
Final eccentricity vs final semi-major axis (in AU) for a Phobos-like object after binary disruption. The graph only shows those results obtained where SMA are smaller than 0.04 AU, and eccentricities lower than 1.15. Different colours are used to represent results obtained for different masses of the binary companion, for 24 different combinations of velocity at infinity and binary SMA parameters.

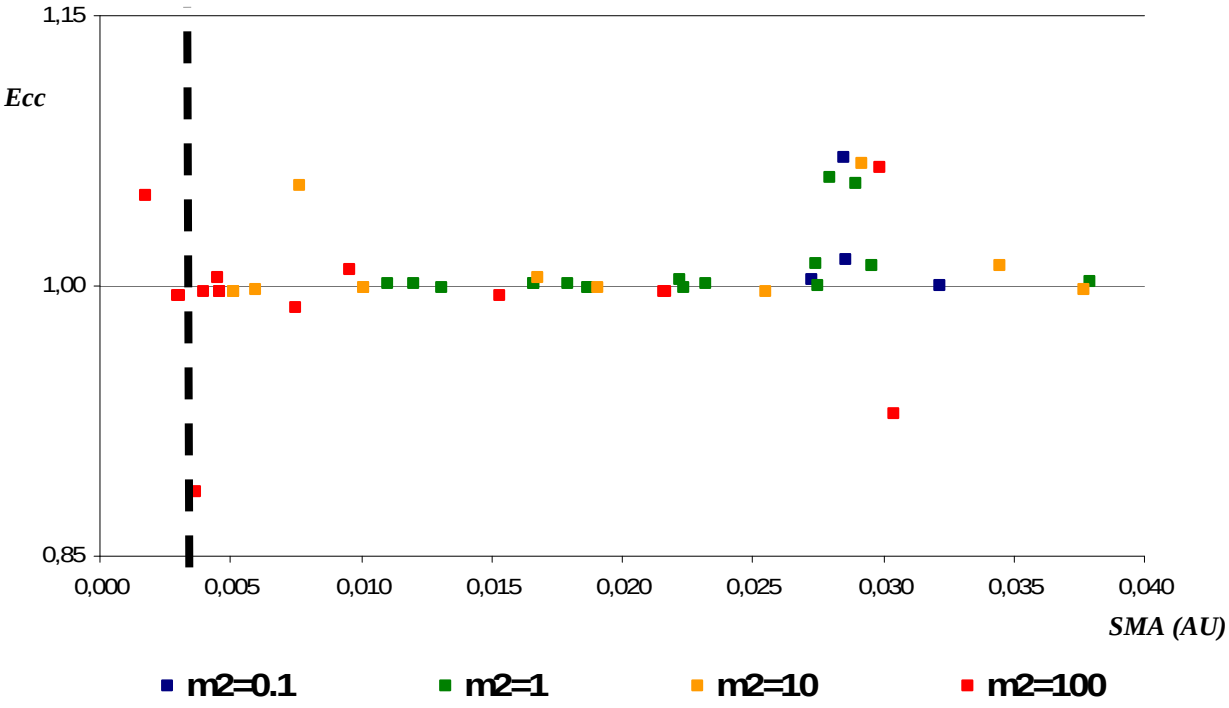

Figure 10
The same 'e vs a' graph as previous figure but for another 96 simulations. This time the hyperbolic approaching trajectory was forced to pass nearer Mars, while all other parameters remained the same. The scale of this plot exactly matches the previous one.

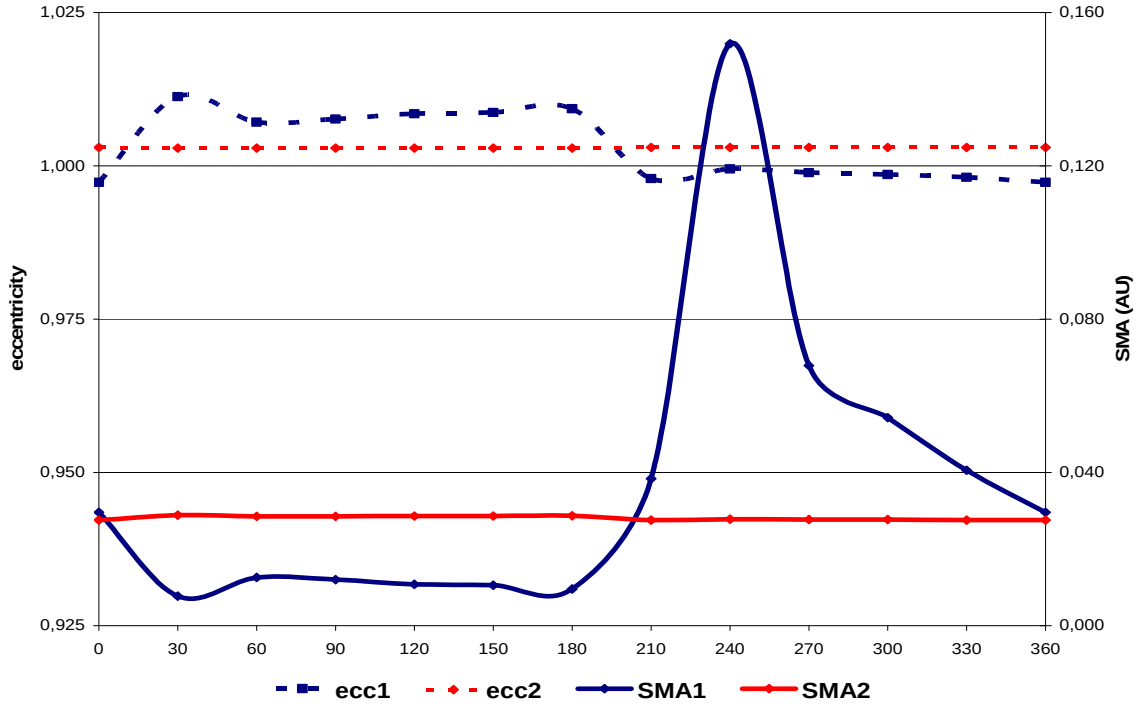

Figure 11
The orbital phase case for = 100 m/s, a_{bin} = 20 R_{Phob}, m_2 = 100 M_{Phob}.
For those angular positions where $e_1 < 1$, always $a_1 > 0.0036$ AU, so that no permanent capture is possible. Given the large mass of the companion, both its a_2 and e_2 practically does not vary at all.

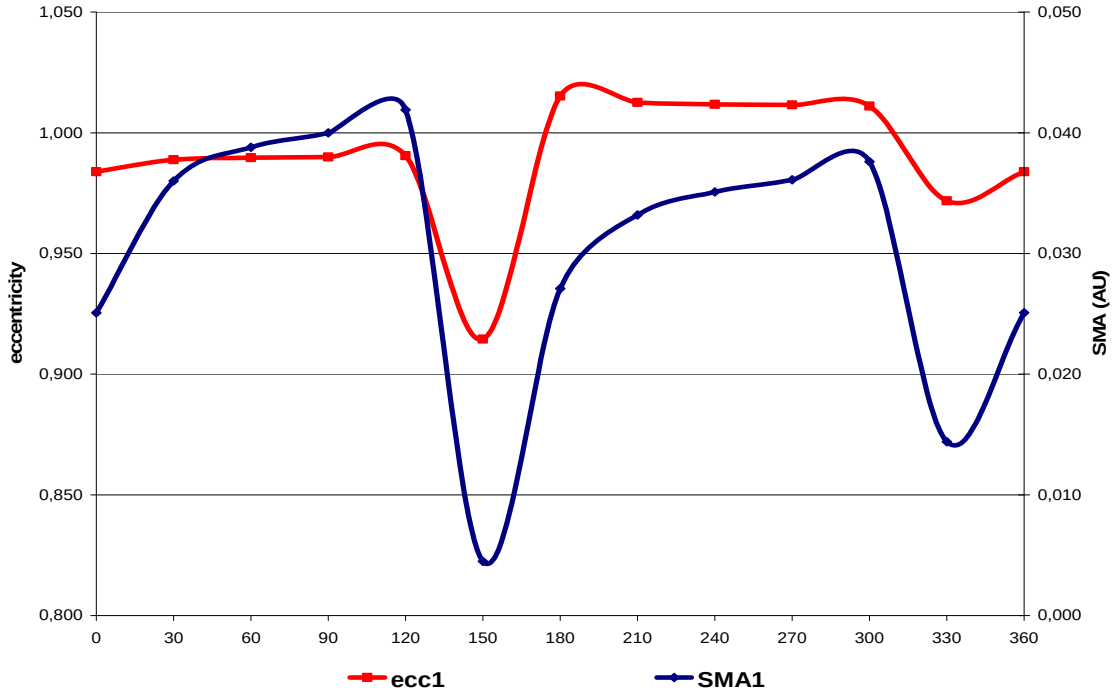

Figure 12
The orbital phase case for = 6.4 m/s, a_{bin} = 20 R_{Phob}, m_2 = 10 M_{Phob}.
For clarity sake, curves for companion object have been omitted. About 150° it is observed an abrupt decrease for both object # 1 curves; anyway, permanent capture is not possible because still $a_1 > 0.0036$ AU.

Despite having tried with v_∞ values much lower than those used for Triton's case, and also approaching Mars from closer binary trajectories, practically no favourable combination of parameters for a permanent capture of a Phobos-like object was found. Two factors concur for such outcome: (i) the relative low mass of the red planet (160 times lower than Neptune's) which makes its gravitational potential energy simply too weak for overcoming kinetic energies of approaching binary members, and (ii) the relative nearness of the Sun (only 5 % of Neptune's semi-major axis) which makes its Hill sphere too small for completely containing the large orbits of those transitorily captured objects.

Deimos' case

Figure 13 presents the final eccentricity versus final semi-major axis for a Deimos-like object obtained from the performed 96 simulations, although only showing those results with lowest eccentricities and SMAs. Not surprisingly, given that Deimos is physically alike Phobos (about 20% lesser mass, 50% lesser diameter), the graph is very similar to those obtained from Phobos' cases. Again, no permanent captured cases were found.

Simulations for both Martian moons have been run covering a wide range of potential binary asteroids: the full spectrum for expected velocity at infinity, three orders of magnitude for the mass of the companion, and more than two orders of magnitude for the binary semi-major axis. Nevertheless, no cases were found to support the idea that Martian satellites were captured by means of a binary-planet gravitational encounter.

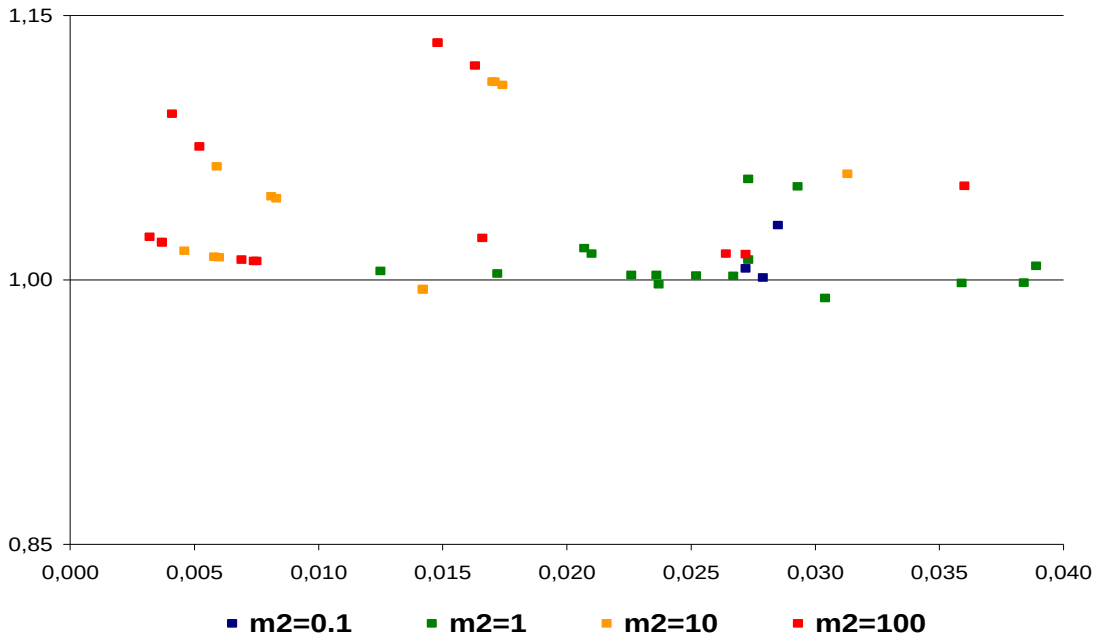

Figure 13
Final eccentricity vs final semi-major axis (in AU) for a Deimos-like object after binary disruption. The graph only shows those results obtained where SMA are smaller than 0.04 AU, and eccentricities lower than 1.15. Different colours are used to represent results obtained for different masses of the binary companion, for 24 different combinations of velocity at infinity and binary SMA parameters.

Conclusions

Capture of irregular satellites is still one major topic in modern Solar System dynamics. Recently, the 'old' capture model by three-body interactions has been improved by considering binary-planet encounters – where the required energy dissipation comes from the slow speeds relative to the planet that each one of the binary objects transitorily experiences during part of their revolution around the common centre of mass.

In order to investigate the viability of binary-planet gravitational encounters as the likely mechanism for general satellite capture, computational analysis was applied to the three particular cases that seem to lie at the Antipodes of the satellite scale: Triton, Phobos and Deimos. For each one, simulations roughly covering a wide spectrum of potential binary characteristics were performed.

Results for Triton have been highly auspicious, as the simulations have showed a broad range of favourable binary characteristics that would have ended in the capture of a Triton-like object. On the contrary, results for both Phobos and Deimos have shown capture by binary-planet encounters almost unviable due to Mars' low mass and small Hill sphere.

This outcome clearly controverts Agnor & Hamilton's optimism about the binary-planet gravitational encounter model becoming the very likely mechanism for explaining virtually all satellite captures in the Solar System. Specifically for the Martian satellites, transitory captures due to binary disruptions could have been the trigger for their origin, but at least some other mechanism necessarily had to act in order to provoke their permanent captures.

References

Agnor, Craig B. and Hamilton, Douglas P., 2006, *"Neptune's capture of its moon Triton in a binary-planet gravitational encounter"*. Nature, Vol. 441, 11 May 2006, pages 192-194

Colombo, Giorgio and Franklin, Fred A., 1971, *"On the formation of the outer satellite groups of Jupiter"*. Icarus, Vol. 15, pages 186-189

Gladman, Brett, and Duncan, Martin, and Candy, Jeff, 1991, *"Symplectic Integrators for Long-Term Integrations in Celestial Mechanics"*. Celestial Mechanics and Dynamical Astronomy, Volume 52, pages 221-240

Gomes, R., Levison, H. F., Tsiganis, K., and Morbidelli, A., 2005, *"Origin of the cataclysmic Late Heavy Bombardment period of the terrestrial planets"*. Nature, Vol. 435, 26 May 2005, pages 466-469

Hahn, Joe, 2005, *"When giants roamed"*. Nature, Vol. 435, 26 May 2005, pages 432-433

Heppenheimer, T. A. and Porco, Carolyn C., 1977, *"New contributions to the problem of capture"*. Icarus, Vol. 30, pages 385-401

Jewitt, David and Sheppard, Scott S., 2005, *"Irregular satellites in the context of planet formation"*. Space Science Reviews, Vol. 116, pages 441-455

Levison, Harold F., and Duncan, Martin J., 1994, *"The Long-Term Dynamical Behavior of Short-Period Comets"*. Icarus, Vol. 108, pages 18-36

Morbidelli, Alessandro, 2006, *"Interplanetary kidnap"*. Nature, Vol. 441, 11 May 2006, pages 162-163

Murray, Carl D., and Dermott, Stanley F., 1999, *"Solar System Dynamics"*. Cambridge University Press, pages 448 and 470

Pollack, James B., Burns, Joseph A., and Tauber, Michael E., 1979, *"Gas drag in primordial circumplanetary envelopes: A mechanism for satellite capture"*. Icarus, Vol. 37, pages 587-611

Selby Cull, 2006, *"Minor Planets Stick Together"*. Sky & Telescope, October 2006, page 20

Sheppard, Scott S., 2005, *"Outer irregular satellites of the planets and their relationship with asteroids, comets and Kuiper Belt objects"*. Asteroids, Comets, Meteors, *Proceedings IAU Symposium* No. 229

Sheppard, Scott S., Jewitt, David and Kleyna, Jan, 2004, *"A survey for outer satellites of Mars: Limits to completeness"*. The Astronomical Journal, Vol. 128, 2004 November, pages 2542-2546

Singer, S. Fred, 2003, "*Origin of Phobos and Deimos: A New Capture Model*". Sixth International Conference on Mars, July 20-25, 2003, Pasadena, California, USA

Stephens, D. C., and Noll, K. S., 2006, *"Detection of six trans-neptunian binaries with NICMOS: A high fraction of binaries in the cold classical disk"*. The Astronomical Journal, Vol. 131, pages 1142-1148

Wisdom, Jack, and Holman, Matthew, 1991, *"Sympletic Maps for the N-Body Problem"*. The Astronomical Journal, Vol. 102, Number 4, October 1991, pages 1528-1538